Electronic Supplementary Information

Improved polarization and endurance in ferroelectric $Hf_{0.5}Zr_{0.5}O_2$ films on $SrTiO_3$(110)

Tingfeng Song, Huan Tan, Saúl Esnadía, Jaume Gàzquez, Martí Gich, Nico Dix, Ignasi Fina,* and Florencio Sánchez*

Institut de Ciència de Materials de Barcelona (ICMAB-CSIC), Campus UAB, Bellaterra 08193, Spain

E-mail: ifina@icmab.es; fsanchez@icmab.es

S1: Simulation of Laue oscillations.

XRD θ-2θ scans of HZO/LSMO/STO(001) and HZO/LSMO/STO(110) samples and shown in Figure S1a and S1b, respectively. The o-HZO(111) reflection is simulated (red curves) according to the equation.[1]

$$I(Q) = \left(\frac{\sin\left(\frac{QNc}{2}\right)}{\sin\left(\frac{Qc}{2}\right)} \right)^2$$

where $Q = 4\pi\sin(\theta)/\lambda$ is the reciprocal space vector, N the number of unit cells along the out-of-plane direction and c the corresponding lattice parameter. The fitting curves were simulated considering peak position $2\theta = 30.067$ ° and thickness of 65 Å (N = 22 and c = 2.972 Å), for the film on STO(001), and $2\theta = 30.339$° and thickness of 65 Å (N = 22 and c = 2.946 Å) for the film on STO(110).

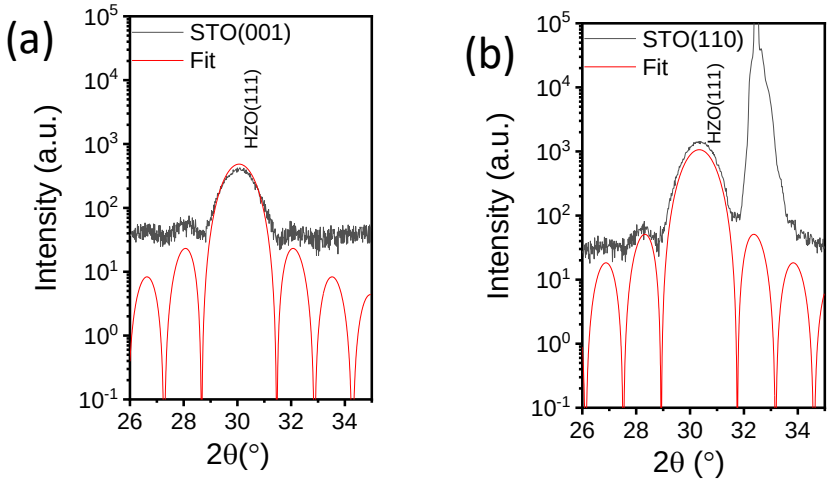

Figure S1. XRD θ-2θ scans of HZO/LSMO/STO(001) (a) and HZO/LSMO/STO(110) (b) samples. Red curves are simulations of Laue oscillations.

S2: Piezoresponse force microscopy amplitude images

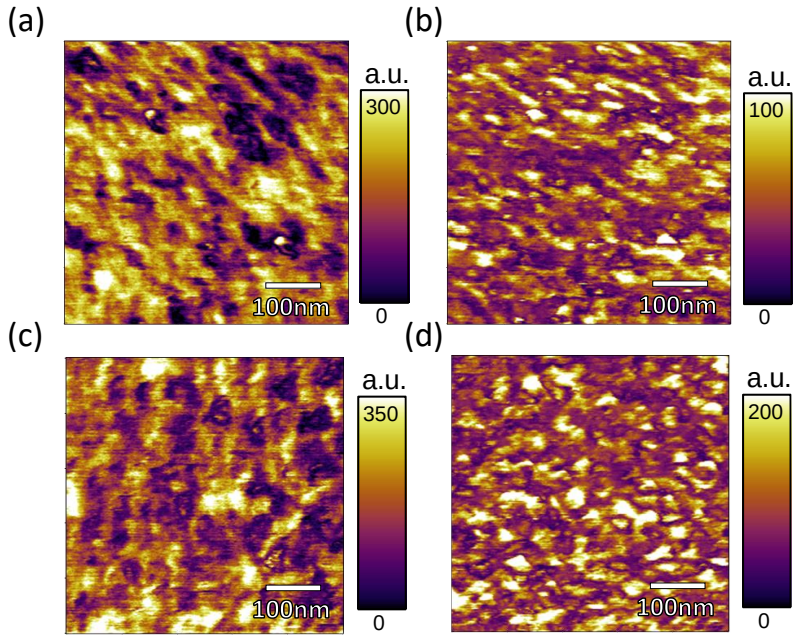

Figure S2. (a) Vertical and (b) in-plane amplitude contrast for the HZO/LSMO/STO(001) sample. (c) Vertical and (d) in-plane amplitude contrast for the HZO/LSMO/STO(110) sample. PFM amplitude images correspond to the phase images shown in Figure 1c,d and Figure 1e,f, respectively.

S3: Sketches of the epitaxial relationships between crystal variants and substrates

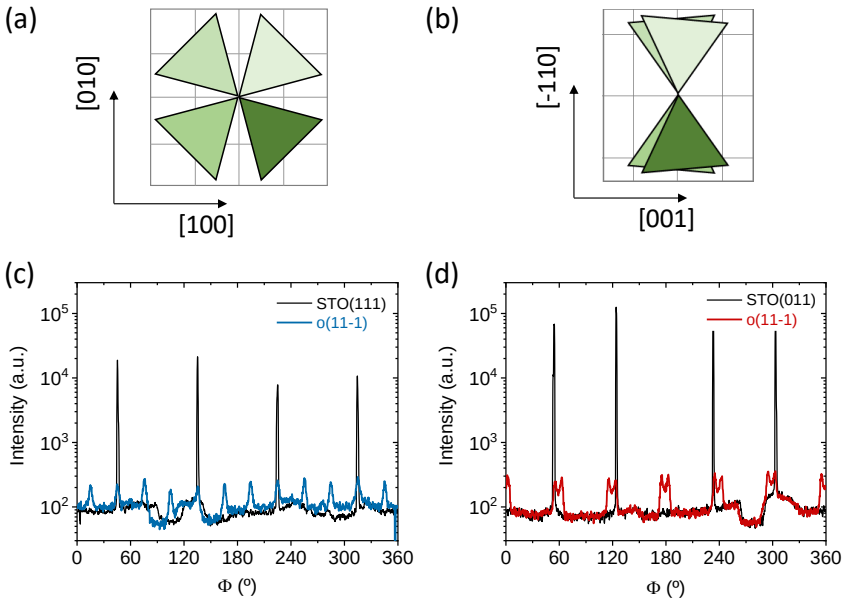

Figure S3. (a,b) Sketches of the HZO crystal domains respect the substrates cells for films grown on STO(111) and STO(110), respectively . (c,d) ϕ-scans extracted from pole figures for the films grown on STO(111) and STO(110), respectively. The STO(111) and STO(011) scans are plotted in black, and the o-{11-1} families are plotted in blue (c) and red (d). The o-{11-1} peaks were integrated for ϕ between 2θ = 29.8-30.6° and χ = 65-75°.

S4: STEM: Simultaneous ABF and HAADF images

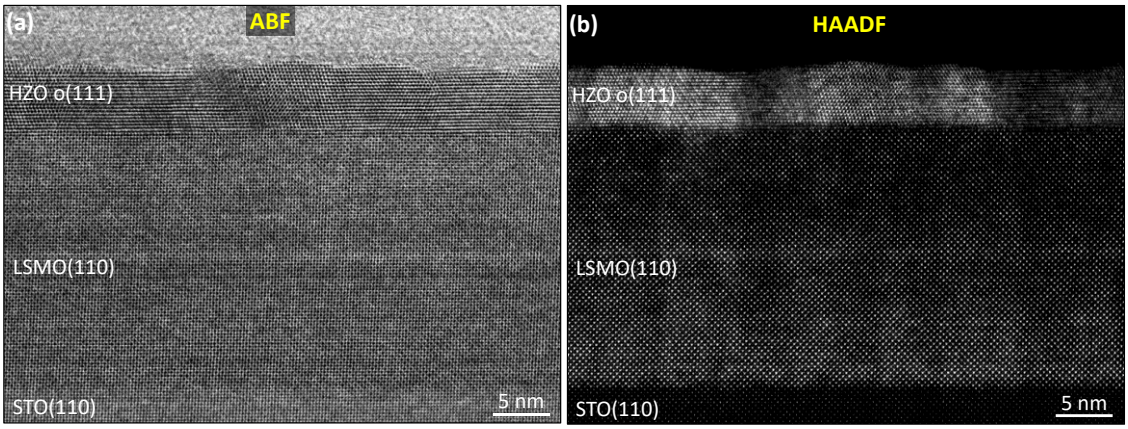

Figure S4. (a-b) Simultaneously acquired annular bright field (ABF) (a) and high-angle annular dark field (HAADF) (b) cross-sectional images corresponding to the image shown in Figure 3 of the main text. From bottom to top, the STO(110) substrate, the LSMO(110) electrode and the HZO(111) film can be appreciated.

S5: Top view of HZO(111) on LSMO(110)

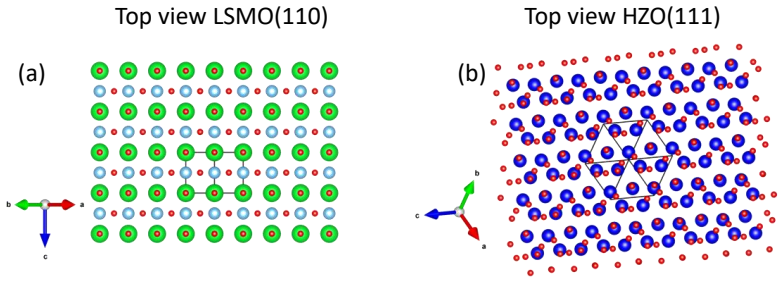

Figure S5. (a) Top view of LSMO(110). Red, green and turquoise balls correspond to oxygen, La/Sr and Mn atoms. (b) Top view of HZO(111). Red and blue balls correspond to oxygen and Hf/Zr atoms. The visualization of the showed structures was done in VESTA.[2]

S6: STEM characterization (reconstructed image from reflections in the Fourier space)

In domain lattice mismatch (DME), m lattice planes of the film match with n (n = m ±1) lattice planes of the substrate (or bottom layer), in contrast with the one-to-one matching in conventional epitaxy. The size of the domains, fixed by m, depends on the lattice parameters, and permits to reduce the lattice mismatch to a low value. Typically domains of different size (different m) coexist; some of them presenting positive mismatch and some others presenting negative mismatch.[3] The coexistence allows that the overall mismatch is null. In the epitaxy of HZO on LSMO/STO(110) here studied, there is low mismatch for a range of domain sizes. Considering the lattice parameter of STO (LSMO is strained) the lowest mismatch corresponds to m = 9 and n = 10:

$$\left(\frac{(9 \cdot 2.76) - (8 \cdot 3.118)}{(8 \cdot 3.118)}\right) = \mathbf{-0.41}\ \%$$

and there is low mismatch in a wide range of m/n domains ranging from 6/7 (f = + 3.7 %) to 11/12 (f = - 3.0 %). The filtered STEM image (Figure S6b) shows the presence of these domains.

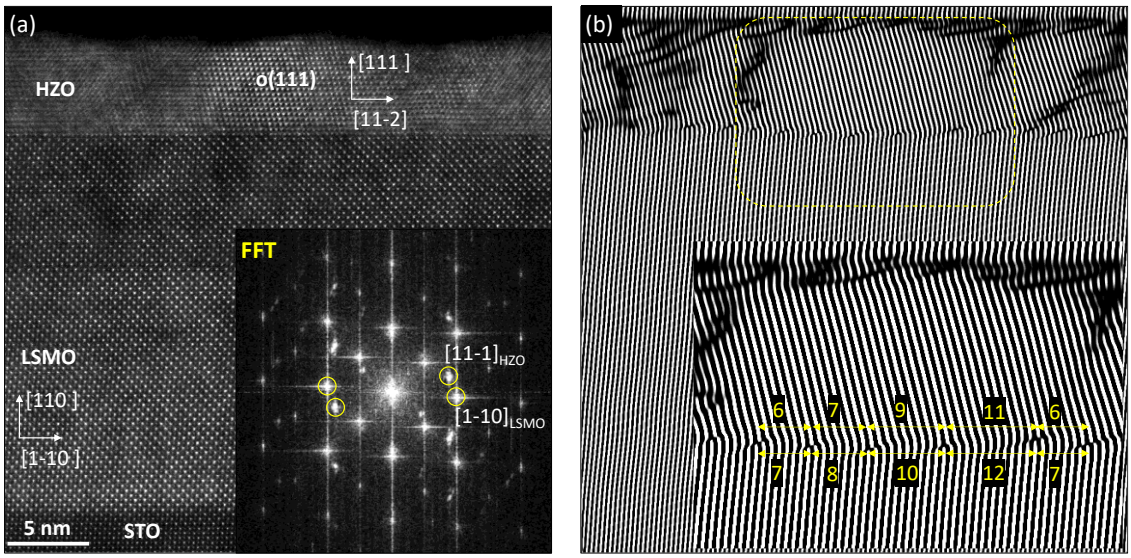

Figure S6. (a) Cross section high angle annular dark field STEM image of HZO/LSMO/STO(110). The inset show the Fast Fourier Transform (FFT). The marked reflections in the FFT were computed in the inverse FFT to obtain the filtered image in (b). (11-1) planes of HZO are used since these planes end in the Hf/Zr cations at the interface, while (11-2) planes do not.

S7: Atomic force microscopy image of the HZO/LSMO/STO(110) sample

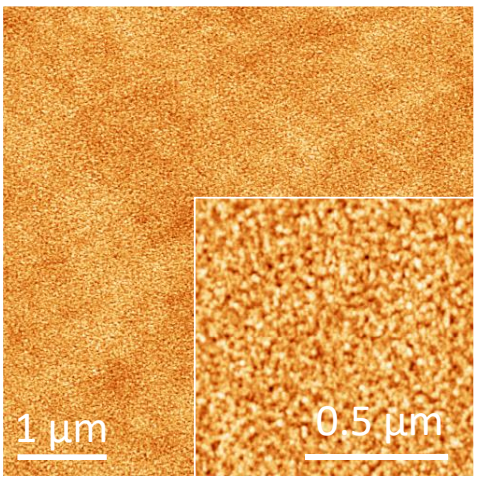

Figure S7. Topographic AFM image of a 5 µm x 5 µm region of the HZO/LSMO/STO(110) sample. The root mean square roughness is 0.25 nm. The inset at the bottom left shows the image of a 1 µm x 1 µm region.

S8: Leakage curves during endurance tests

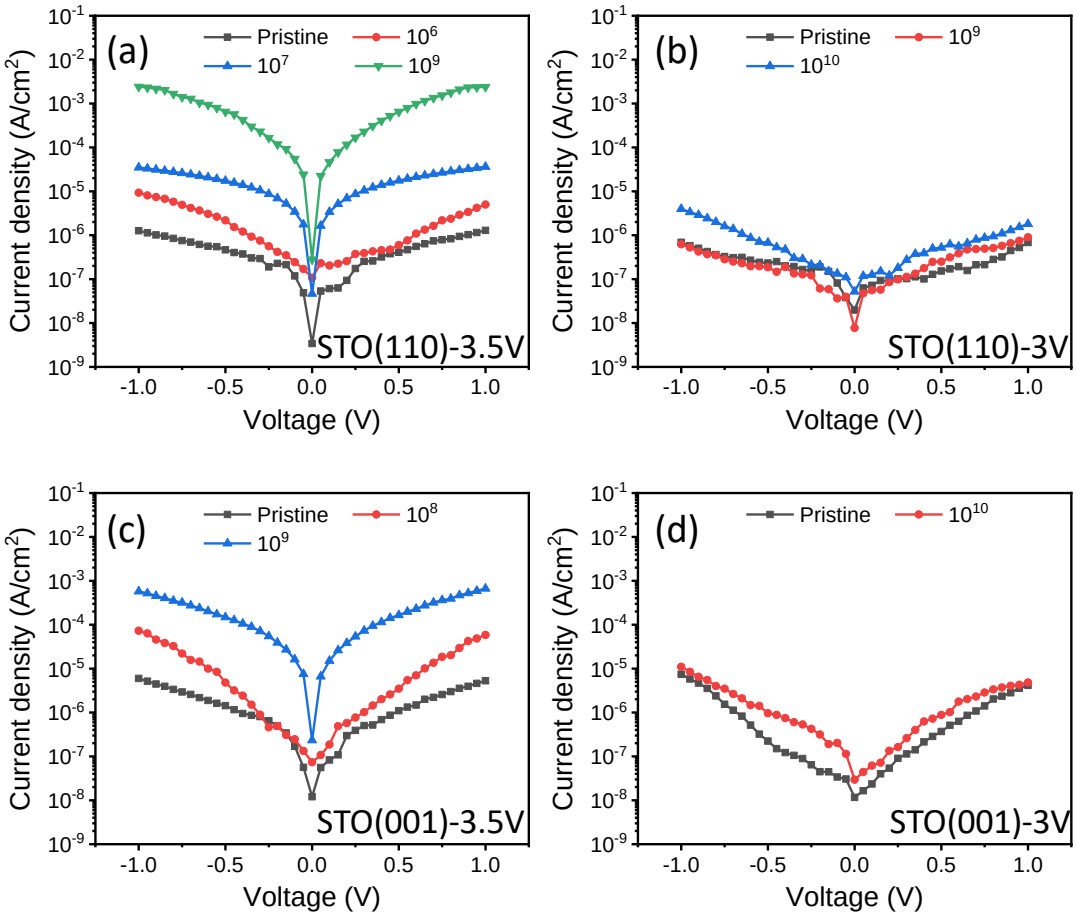

Figure S8. Current leakage density vs electric field characteristics of the pristine state and after the indicated number of bipolar cycles for the HZO/LSMO/STO(110) sample at 3.5 V (a) and 3 V (b), and for the HZO/LSMO/STO(001) sample at 3.5 V (c) and 3 V (d).

S9: Polarization loops during endurance tests

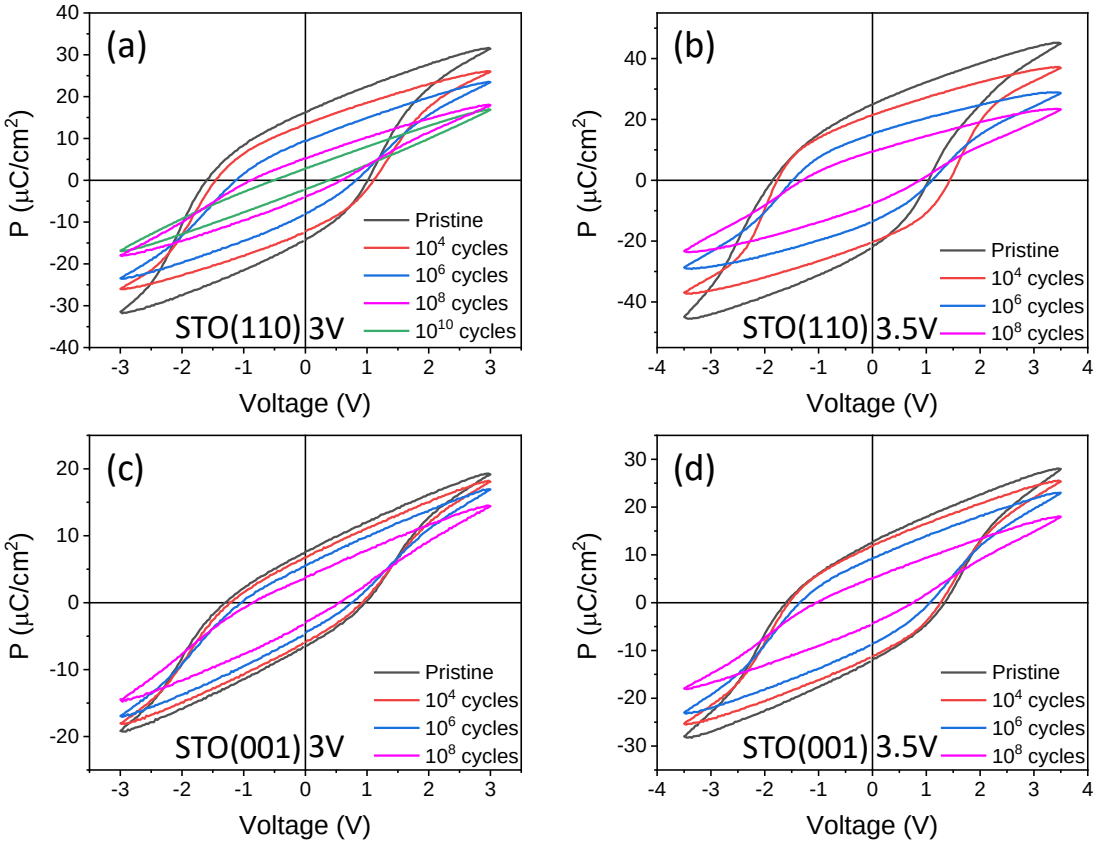

Figure S9. Polarization loops vs voltage characteristics of the pristine state and after the indicated number of bipolar cycles for the HZO/LSMO/STO(110) sample at 3 V (a) and 3.5 V (b), and for the HZO/LSMO/STO(001) sample at 3 V (c) and 3.5 V (d).

References

1 J. Lyu, I. Fina, R. Solanas, J. Fontcuberta and F. Sánchez, *Appl. Phys. Lett.*, 2018, **113**, 082902.

2 K. Momma and F. Izumi, *J. Appl. Crystallogr.*, 2011, **44**, 1272.

3 S. Estandía, N. Dix, M. F. Chisholm, I. Fina and F. Sánchez, *Cryst. Growth Des.*, 2020, **20**, 3801.